Aftershocks, Seismic Efficiency, and Fluid Diffusion for the Cooper Basin (Australia) Geothermal Stimulation

Enrico Caffagni*, Florian Fuchs, and Götz Bokelmann (IMGW, Althanstraße 14 UZA II, 1090 Vienna, Austria)

1 Introduction

Long-term fluid-injection experiments have been conducted in geothermal fields in the Cooper Basin (Australia). Habanero 1 was the first well drilled into the granitic fabric [3] at a bottom depth of approximately 4.4 km. Successively six other wells have been drilled [2]. Fluid injection has generated large amounts of induced seismicity.

We have acquired a data package from the Government of South Australia, and analyzed catalogs of the seismicity that has occurred within a time interval between 2003 and 2013. Table 1 shows details of the detected seismicity for each stimulation stage (hereafter called "stages"), and Figure 1 the relative location to the Habanero 1 well.

Seismicity detected in the Cooper Basin (2003-2013)

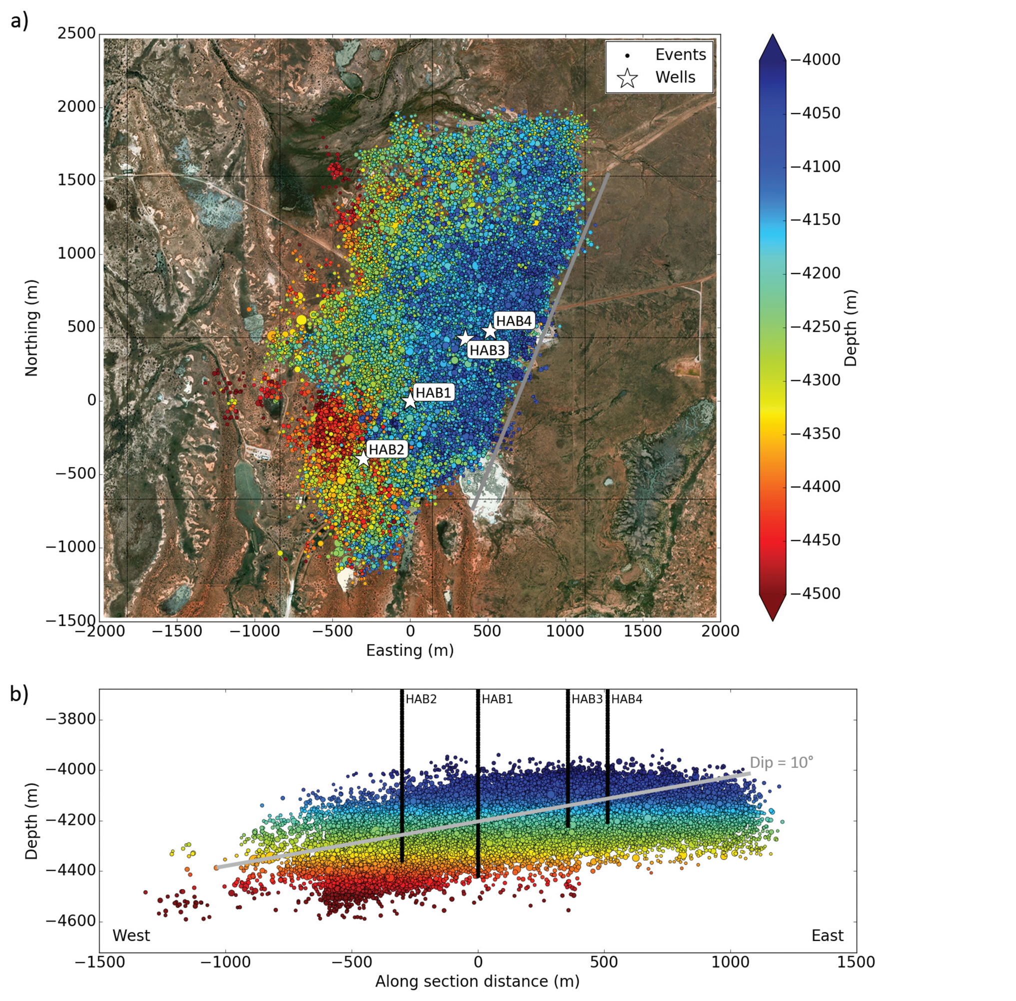

Figure 1: Seismicity (top view, panel a) extends up to the eastern line striking NNE-SSW (from [5]). EW vs depth section of the seismicity (panel b) exhibits the presumed triggered tectonic structure, which dips to W (seismicity from the Jolokia well not shown here).

Stage name	Seismicity duration	N. earthquakes (locatable)	Magnitude range
Habanero 1	6/11/2003 - 6/4/2005	23459	[-2.0,3.7]
Habanero 1-2	21/7/2005 - 11/11/2005	8873	[-1.0,2.9]
Habanero 3	17/4/2008 - 18/4/2008	310	[-1.5,1.7]
Jolokia 1	23/10/2010 - 4/12/2010	131	[-1.2,1.4]
Habanero 4	10/11/2012 - 4/12/2012	20735	[-1.5,3.0]
Habanero 4 post	4/12/2012 - 23/1/2013	1048	[-1.4,1.8]

Table 1: Details of the detected induced seismicity for each stimulation stage in the Cooper Basin, obtained from the catalogs provided by the Energy Resources Division (South Australia Government).

2 Objectives

1. **Check the existence of aftershocks for induced events**
2. **Evaluate the seismic response of the reservoir as a function of the injection history**
3. **What causes and controls the seismicity? How does fluid mainly diffuse - volumetric (3D) or planar (channel flow)?**

3 Methods

Each method number corresponds to the objective number.

1. **Relative locations of time-consecutive events (RLCE)**
   The n^{th} RLCE gives the spatial separation between the $(n{+}1)^{st}$ and n^{th} location. To each n^{th} RLCE pair the magnitude of the n^{th} event has been associated.
2. Mainshocks found for each stage, then computed the seismic moment M_0, and associated it to the corresponding value of the cumulative injection volume ΔV, as in [6].
   Seismic efficiency defined as the ratio of the cumulative M_{0cum} (measured) to the total expected M_{0t} release [4], which [6] showed to be directly connected to ΔV:
   $$\sum M_{0t} = 2G\Delta V \quad . \tag{1}$$
3. **"2D fluid front"** (fluid distribution) defined for seismicity expected to occur on a localized single fault or fracture plane (2D):
   $$r_{2D}(t) = \sqrt{\frac{Q_I t}{2w(t)}} \quad . \tag{2}$$
   Q_I is the injection rate; $w(t)$ is the fracture width (aperture), depending on the injection time. Assumed a penny-shape circular crack and negligible fluid loss.
   r-t plot [7] used to infer fracture growth, as the maximum extent of seismicity.
   Finally compared the 2D front to $\sqrt{4\pi Dt}$ (3D) fluid diffusion, with D hydraulic diffusivity, in relation also to the injection history.

4 Results

4.1 The "Christmas-tree" effect

Space patterns of the RLCE

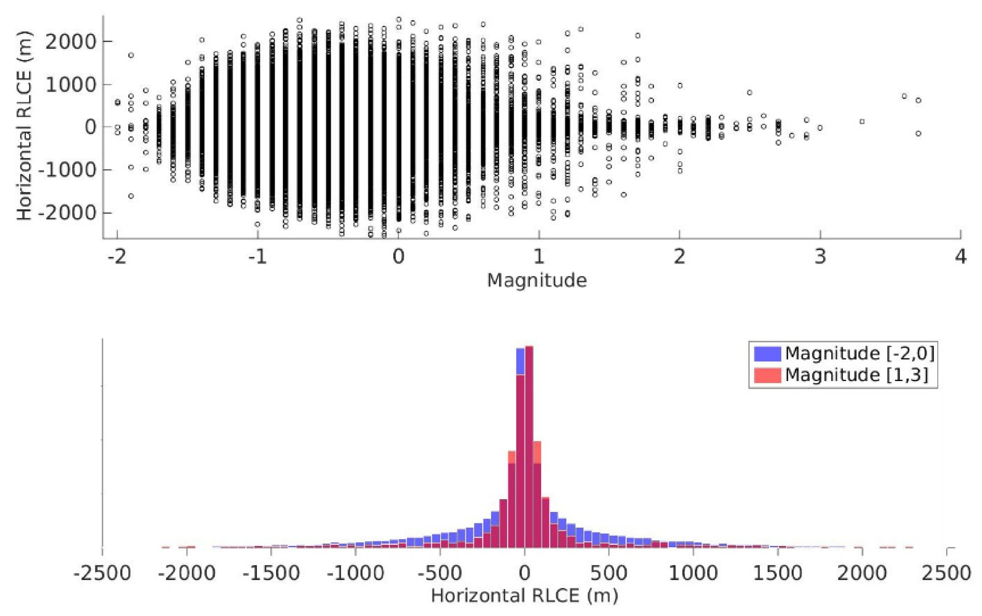

Figure 2: RLCE pairs as a function of magnitude (of the first event in the pair) for the horizontal component (top panel). RLCE comprise the entire stimulation period from 2003 to 2013. Bottom panel shows the statistical distribution of the RLCE for two magnitude ranges (lower and higher). The two distributions are clearly different, indicating that the Christmas-tree effect is not due to the different number of events.

RLCE shape striking!
Smaller event separation towards higher magnitudes.
We call this the "Christmas-tree" effect. Is it real?

RLCE distributions at lower and higher magnitude are different. The effect is real! What are the causes?
We propose the existence of aftershocks from mainshocks with magnitude in the range of 1 to below 4.
Aftershocks decay in time following the Omori law. Our aftershocks?

Time patterns of the RLCE

Figure 3: Number of events as a function of time, 6 hours after the larger events identified for each stage, as well the corresponding RLCE for the two magnitude ranges as in Figure 2.

Yes. For some of them an Omori-like behavior is recognizable

4.2 Seismic efficiency: "Triggered" or "Induced"?

McGarr' and efficiency plot

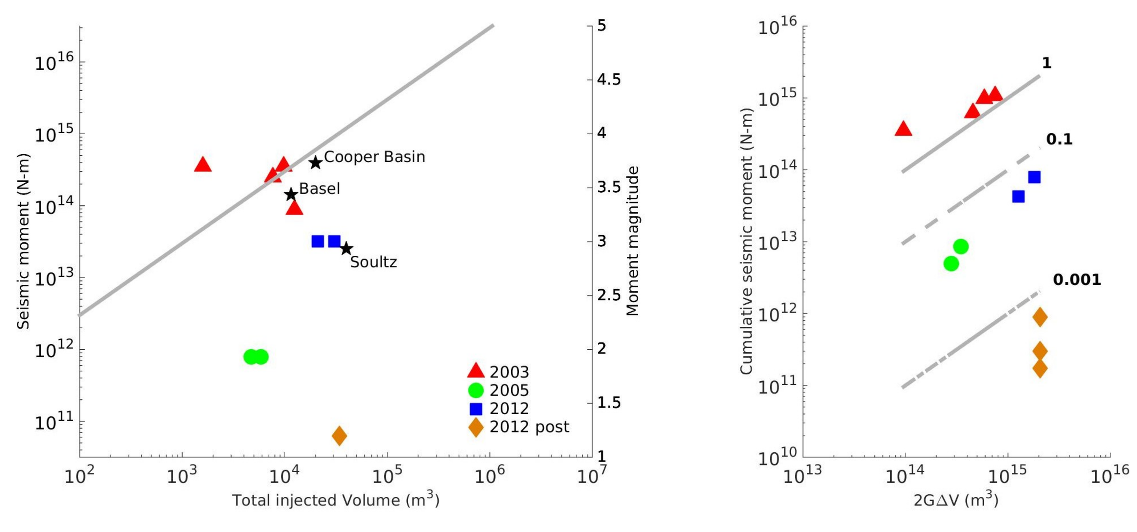

Figure 4: McGarr' plot (right). The events of the 2003 stage are the same as in Figure 3, for the other stages only the largest mainshocks have been represented. The oblique line defines the threshold of the McGarr' model, and gives the predicted seismic moment for a given injected volume, assumed to be distributed equally in a 3D space. A few case histories are also taken from McGarr (2014) including a Cooper Basin case. Left panel shows M_{0cum} versus $2G\Delta V$. The numbers give the seismic efficiency. Oblique lines represent thresholds of the partitioning.

Some of the 2003 events (Habanero 1) are above the predicted seismic moment from the McGarr' model!
There are two possible explanations:

(a) **Some events are "triggered" rather than "induced"**
(b) **Injected volume may not have been the controlling factor, rather was the available fault size, as already argued by [1]**

4.3 Fluid diffusion

r-t plot for Habanero 1 stage (2003 year)

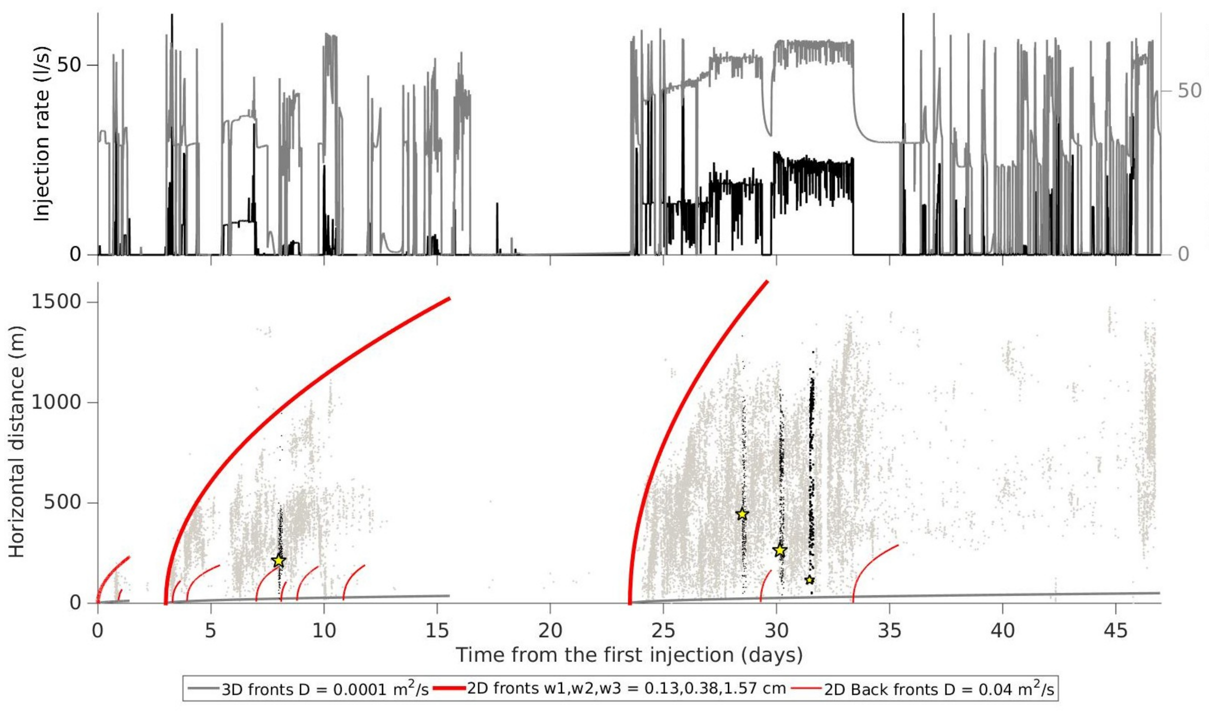

Figure 5: Top panel shows the injection curves. Bottom panel displays the r-t plot. Plotted are the 2D fluid front curves for 3 different values of w as in eq. 2, and multiple back fronts of the seismicity as in [7], according to the ends of injection intervals. The 2D front curves can be obtained from the 3D triggering fronts with D values equal to 0.0351, 0.1696, and 0.3906 m^2/s. In addition, 3D fronts are plotted with a more realistic value of D. Stars denote the mainshocks of Figure 3. Black dots identify the aftershock sequences within 4 hours from the mainshocks.

- **Fracture growth inferred: 200 m at day 1 up to 1200 m at day 27**
- **Clear correlation between seismicity and 2D fluid fronts, and between the back fronts, interpreted as closing of the fractures occurring mainly during shut-in times**
- **Reasonable values of the fracture width *w*, they increase progressively from the first injection**
- **Correlation between the maximum extent of the fractures and aftershock growth**

Have pore pressure-effects alone controlled the seismicity? No!
Flow rate on faults: main triggering mechanisms

Fluid mainly distributes in a channel (2D). The more the flow rate increases, the more the fractures open, which favors shearing. Stimulated critically pre-stressed fractures trigger mainshocks "creating" new pathways for the fluid, inducing later events. Aftershocks (induced) could be the slippage of part of the induced fracture network "body".

5 Conclusions

- Analyzing consecutive event pairs, we have identified a peculiar dependence of event locations on magnitude, which we call "Christmas-tree". We have interpreted this effect as due to aftershock behavior occurring for induced seismic events in the magnitude range of 1 to 3.5.
- Different degrees of seismic efficiency in the basin have revealed a different behavior for the different stages. The seismic efficiency could be used to infer earlier "triggered" from later "induced" events.
- For the Cooper Basin, fluid diffuses on a plane (2D).
  Flow-rate dependent effects occurring on the fractures, which respond to the injection, are important for triggering the seismicity.
  Linear pore pressure diffusion alone are not sufficient.
  Larger seismic events generate big fractures, creating new pathways for the fluid flow, and extends the seismicity in forms of aftershocks.

References

[1] Gail M. Atkinson, David W. Eaton, Hadi Ghofrani, Dan Walker, Burns Cheadle, Ryan Schultz, Robert Shcherbakov, Kristy Tiampo, Jeff Gu, Rebecca M. Harrington, Yajing Liu, Mirko van der Baan, and Honn Kao. Hydraulic Fracturing and Seismicity in the Western Canada Sedimentary Basin. *Seismol. Res. Lett.*, 87(3):1–17, 2016.

[2] Stefan Baisch, Elmar Rothert, Henrik Stang, Robert Vörös, Christopher Koch, and Andrew McMahon. Continued Geothermal Reservoir Stimulation Experiments in the Cooper Basin (Australia). *Bull. Seismol. Soc. Am.*, 105(1):198–209, 2015.

[3] Stefan Baisch, Ralph Weidler, Robert Vörös, Doone Wyborn, and Lambertus de Graaf. Induced Seismicity during the Stimulation of a Geothermal HFR Reservoir in the Cooper Basin, Australia. *Bull. Seismol. Soc. Am.*, 96(6):2242–2256, 2006.

[4] L. Buijze, B. Wassing, P.A. Fokker, and J.D. van Wees. Moment Partitioning for Injection-Induced Seismicity: Case Studies and Insights from Numerical Modeling. pages 1–11, 2015. Melbourne, Australia, 19-25 April 2015.

[5] Heinz-Gerd Holl and Colleen Barton. Habanero Field - Structure and State of Stress. pages 1–5, 2015. Melbourne, Australia, 19-25 April 2015.

[6] A. McGarr. Maximum magnitude earthquakes induced by fluid injection. *J. Geophys. Res.: Solid Earth*, 119(2):1008–1019, 2014.

[7] S.A. Shapiro and C. Dinske. Fluid-induced seismicity: Pressure diffusion and hydraulic fracturing. *Geophys. Prospect.*, 57(2):301–310, 2009.

Acknowledgements

We thank the FracRisk community (www.fracrisk.eu). The project has received funding from the EU's Horizon 2020 research and innovation programme under grant agreement No 636811.

We thank greatly the Government of South Australia for providing the dataset.

The paper benefited from discussions with S. Baisch and R. Jung.